Introducing ductility in hybrid carbon fibre/self-reinforced composites through control of the damage mechanisms

Yentl Swolfs*[1], Yannick Meerten[1], Peter Hine[2], Ian Ward[2], Ignaas Verpoest[1], Larissa Gorbatikh[1]

[1] Department of Materials Engineering, KU Leuven, Kasteelpark Arenberg 44 bus 2450, 3001 Leuven, Belgium
[2] Soft Matter Group, University of Leeds, LS2 9JT, United Kingdom
*Corresponding author: yentl.swolfs@mtm.kuleuven.be, Tel.: 0032 16 37 36 16

Abstract

Carbon fibre composites possess excellent mechanical properties, but suffer from brittleness. Hybridisation with self-reinforced polypropylene (SRPP) is a promising strategy to introduce ductility into carbon fibre-reinforced polypropylene (CFRPP). The present work demonstrates how different damage mechanisms in these hybrid composites change as a function of the carbon fibre volume fraction, the directionality of CFRPP and SRPP and their relative layer thickness. Multiple fractures of the CFRPP layers or "fragmentation" is achieved by optimising these parameters. This leads to a ductile hybrid composite with a gradual failure development.

Keywords: Hybrid composites; Delamination; Self-reinforced composites; Ductility

1 Introduction

Carbon fibre-reinforced composites combine excellent mechanical properties with a low density. This makes them a preferred choice in many lightweight structural applications. Their main drawback however, is a low tensile failure strain due to the intrinsic brittleness of the reinforcing fibre. One solution is to replace the carbon fibres by fibres with a larger failure strain, such as polymer [1-3] or metal fibres [4, 5]. This solution is compromised by accompanying disadvantages, such as lower strength and increased temperature sensitivity of polymer fibres and much higher density of metal fibres. There is hence a strong need for new ideas on how to improve the failure strain of fibre-reinforced composites.

The basic question is whether a brittle material can be made ductile through intelligent design. An affirmative answer to this question can be found both in naturally occurring and in man-made materials. Biological composites, such as bone and nacre, are known for their remarkable robustness against failure and sophisticated energy absorbing mechanisms [6-8]. Haversian bone, for example, is capable of undergoing high inelastic strains because of its unique microcracking process that gradually develops in its concentric lamellae [9]. Nacre's inelastic deformation is attributed to progressive sliding and stable pull-out of its platelets [10, 11]. In both cases, a well-balanced interplay between microstructural parameters and constituent properties is crucial for the activated damage mechanisms [10].

Among man-made materials, ductile behaviour was successfully achieved in engineered cementitious composites (ECC), also known as bendable concrete [12]. Unlike regular concrete that fails in a brittle manner, due to a single propagating crack initiated at a pre-existing flaw, bendable concrete undergoes excessive cracking over a large volume before it fails. The ductility originates from an accurate control of the opening of these cracks by bridging them with fibres. The design requires tailoring of the fibre size, fibre strength, interfacial strength and the size of the pre-existing flaws. With the correct set of parameters, the mechanism on the tension side of a flexural test is

changed from a single crack propagation to multiple cracking. The result is a failure strain improvement by two orders of magnitude, from 0.01% for standard concrete to 5% for concrete reinforced with polyvinyl alcohol fibres [12].

While the situation in fibre-reinforced polymer composites is different from that in biological composites or fibre-reinforced concrete, certain concepts are universal and can be transferred to the other materials. Two concepts that can be transferred to brittle carbon fibre composites are that (1) a more ductile fibre should be added, and (2) a gradual damage development is achieved through multiple cracking. Fibre hybridisation is a promising approach to achieve these goals. Partial replacement of carbon fibres with a more ductile fibre provides more control over the failure mechanisms. Most hybridisation studies so far have focused on the addition of glass or aramid fibres to carbon fibre composites [13-23].

Another vital parameter in controlling the failure mechanism is the bonding strength between the layers of the hybrid composite. When the carbon fibre layers in an unbonded carbon/glass interlayer hybrid fracture, then delaminations will develop and spread over the entire length of the sample [13]. This leads to a significant vertical load drop, after which the tensile diagram of the hybrid composite resembles that of the glass fibre composite. In the case of a strong bonding however, a more gradual transition from carbon to glass failure is achieved.

Recently, multiple cracking or fragmentation was achieved by sandwiching thin carbon fibre layers between thick glass layers [14]. For thicker carbon fibre layers, the behaviour reverted back to unstable delaminations, similar to that observed by Bunsell and Harris [13]. The fragmentation case however, allowed the carbon fibre layers to break repeatedly, resulting in a sustained stress level. This allowed their hybrid composites to reach ultimate failure strains of up to 2.8% without a drastic load drop. In the same work, an analytical equation was derived to predict the maximum layer thickness that allows this fragmentation [14]. This was later extended to a more refined numerical model in [15]. The material behaviour was referred to as pseudo-ductility, which can be defined as the occurrence of ductility in an inherently brittle material through control of the damage mechanisms. So far, it has only been achieved at low volume fractions of the brittle fibre.

The failure strain improvements that can be achieved by hybridisation with aramid or glass fibres are limited by the low failure strain of these fibres. Large improvements in the ultimate failure strain are only possible through hybridisation with a much tougher fibre [24-26]. This was achieved by hybridisation of carbon fibre with self-reinforced PP (SRPP) [24]. SRPP is a tough material with a high failure strain of about 20% [1, 27]. While this ultimate failure strain was also maintained in the hybrid composites, the carbon fibre failure was accompanied by a significant load drop [24]. SRPP has also shown great potential in fibre-metal laminates, where the presence of SRPP in between aluminium plies led to a more ductile response in impact [28, 29]. The combination of two ductile components in fibre-metal laminates leads to a ductile tensile behaviour without a load drop prior to final failure.

This work aims to understand the parameters governing the failure development in interlayer hybrid composites of carbon fibre and self-reinforced polypropylene. Pseudo-ductility is targeted by controlling the damage mechanisms through an intelligent choice of structural and material parameters. The final purpose is to develop a new material with reasonable stiffness, but with drastically increased ultimate failure strain.

2 Materials and methods

2.1 Materials

Propex Fabrics GmbH (Germany) provided drawn polypropylene (PP) tapes, with a stiffness of 10 GPa and a strength of 500 MPa [3]. The tapes were provided on a bobbin as well as in a twill 2/2 woven fabric with an areal density of 130 g/m². Propex Fabrics GmbH also provided a 50 µm thick PP film for impregnating the carbon fibre weave. This film has a melting point of 163°C and consists of the same PP grade as the drawn PP tapes.

Two types of carbon fibre preforms were used in the study. Unidirectional carbon fibre-reinforced polypropylene (CFRPP) prepregs were sourced from Toray Carbon Fibers Europe (France). These 300 µm thick T700S prepregs have a fibre volume fraction V_f of 45% (see section 2.4).

A balanced spread tow plain weave Textreme 80PW was sourced from Oxeon AB (Sweden). The areal density was 90 g/m², of which 80 g/m² is UTS50S carbon fibre and the rest is epoxy binder. The weave was pre-impregnated in a hot press at 220°C using a single 50 µm PP film. The pressure was alternated between 1 and 10 bar every minute for a total of 10 min, resulting in prepregs with a thickness of 104 µm and a V_f of 43%.

2.2 Composite production

Different interlayer hybrids of SRPP and CFRPP were produced (see Table 1). S and C indicates SRPP and CFRPP layers respectively, while superscripts "w" and "u" indicate woven and unidirectional preforms, respectively. The $S_xC_yS_xC_yS_x$-layups were chosen to yield sufficiently thick samples, while still having a reasonable dispersion of the carbon fibres. This dispersion is known to be important in the performance of hybrid composites [19]. The lowest carbon fibre V_f in each hybrid configuration was achieved by grouping the carbon fibre layers together in a $S_xC_yS_x$-layup. The values of "x" and "y" in these layups were chosen to yield similar thickness and V_f for the SRPP and CFRPP layers in the different configurations.

In case of UD SRPP, the tapes were wound from the bobbin onto a rectangular frame using a winding machine. The machine translates laterally, while the frame rotates. Each translation of the machine creates one S^U layer on the top and one S^U layer on the bottom of the frame. Winding was interrupted at appropriate time intervals to insert the CFRPP prepreg layers. The other layups were made by stacking of the layers.

The hybrid layups were placed in a copper mould and inserted into a preheated press at 188°C. The materials were hot compacted for 5 min at 45 bar pressure, followed by cooling down to 40°C in 5 min.

The CFRPP reference composite was produced using the same process parameters, but at 5 bar pressure instead of 45 bar. This lower pressure reduces material flow out of the mould and thus limits carbon fibre undulations. The higher pressure for layups with SRPP was needed to limit the intrinsic shrinkage of PP tapes during hot compaction.

Table 1: Identification of the layups, with the measured thickness and overall carbon fibre volume fraction. The carbon fibre volume fraction in the loading direction was obtained by dividing the overall fraction by 2 in case of woven CFRPP.

CFRPP	SRPP	Layup	Thickness (mm)	Carbon fibre volume fraction	
				Overall	In loading direction
UD	/	C_5^u	1.38 ± 0.02	44.9 + 1.9%	44.9%
Woven	/	C_{10}^w	1.04 ± 0.02	42.5 + 1.4%	22.4%
/	UD	S_{20}^u	1.57 ± 0.03	0	0
Woven	/	S_{16}^w	2.35 ± 0.01	0	0
UD	Woven	$S^w C^u S^w C^u S^w$	0.90 ± 0.04	29.3 ± 1.2%	29.3%
		$S_3^w C^u S_3^w C^u S_3^w$	1.79 ± 0.03	12.7 ± 1.2%	12.7%
		$S_6^w C^u S_6^w C^u S_6^w$	3.12 ± 0.02	10.1 ± 2.4%	10.1%
		$S_9^w C^u S_9^w$	2.97 ± 0.04	5.0 ± 2.1%	5.0%
Woven	Woven	$S^w C_2^w S^w C_2^w S^w$	0.85 ± 0.03	20.2 ± 1.3%	10.1%
		$S_3^w C_2^w S_3^w C_2^w S_3^w$	1.71 ± 0.03	11.0 ± 1.2%	5.5%
		$S_6^w C_2^w S_6^w C_2^w S_6^w$	3.06 ± 0.06	7.2 ± 0.5%	3.6%
		$S_9^w C_2^w S_9^w$	2.90 ± 0.05	4.7 ± 1.0%	2.3%
Woven	UD	$S_2^u C_2^w S_2^u C_2^w S_2^u$	0.88 ± 0.02	17.6 ± 1.8%	8.8%
		$S_4^u C_2^w S_4^u C_2^w S_4^u$	1.35 ± 0.03	12.2 ± 1.7%	6.1%
		$S_8^u C_2^w S_8^u C_2^w S_8^u$	2.34 ± 0.06	8.4 ± 0.2%	4.2%
		$S_{12}^u C_2^w S_{12}^u$	2.21 ± 0.05	5.5 ± 0.5%	2.8%

2.3 Tensile tests

Quasi-static tensile tests were performed according to ASTM D3039 on an Instron 4505 equipped with a 100 kN load cell. The strain rate was set to 5%/min to allow fracture within a reasonable time. Tensile samples were water jet cut to minimise damage to the sample edges. The sample dimensions were chosen to be 250x15 mm with a 150 mm gauge length, as recommended by the ASTM standard for UD composites. This sample size was also used for the woven composites. Five samples were tested for each layup.

The front face of the samples was monitored during the test using a camera. A speckle pattern was used to calculate the average surface strain over a length of 50 mm in the middle of the specimen. After CFRPP failure, the surface of most samples was damaged and the surface strain could not be measured anymore. The strain in this region was calculated by using the crosshead displacement, and shifting it by a constant value to ensure strain continuity at CFRPP failure. This approach is accurate for two reasons. Firstly, the error is mainly proportional to the load. Since the load is relatively constant after CFRPP failure, the applied correction is accurate over a large strain interval. Secondly, the approach was verified to be accurate on other types of samples without damaged surfaces. The images were also used to track delaminations. The delaminated length was quantified by measuring the brightness difference between intact and delaminated areas.

2.4 Fibre volume fraction measurement

Matrix burn-off tests were performed according to the ASTM D2584 standard to measure the carbon fibre V_f. The PP is heated in a porcelain crucible until the PP matrix ignites. The samples are

then inserted into a muffle furnace for 4h at 450°C, followed by cooling in a desiccator. The content of the crucible is then treated with acetic acid to remove calcium carbonate residue. This treatment is performed in a glass filter, after which the acetic acid is removed by vacuum filtering. The filter containing the fibres is then dried for 1h at 100°C. The carbon fibre weight fraction is calculated from the weight before burn-off and after drying of the filters. This is converted into carbon fibre V_f by assuming a density of 1800 kg/m³ for the carbon fibres and 920 kg/m³ for PP.

3 Results

3.1 Damage mechanisms in hybrid composites

From the introduction it is clear that the damage mechanisms after CFRPP failure need to be controlled to achieve pseudo-ductility in SRPP/CFRPP hybrid composites. These mechanisms depend on a number of parameters, including the stiffness and strength of the SRPP and CFRPP plies, their thicknesses and the interlaminar fracture toughness. A schematic and simplified representation is shown in Fig. 1. If all parameters except the interlaminar fracture toughness are the same, then this toughness dictates the type of failure of the hybrid composite. For a high fracture toughness, the elastic energy released at the CFRPP fracture has no possibility to be dissipated through delamination. It therefore has to be taken up by the surrounding SRPP layers, resulting in extensive SRPP damage or even immediate failure (see Fig. 1a). For a low fracture toughness, the sample delaminates instantly over the entire length and no further stress build-up is possible in the CFRPP layers (see Fig. 1b). The scenario of interest is the one with an intermediate fracture toughness, in which case a small delamination would be allowed (see Fig. 1c-d). Two possibilities can be distinguished in this case: (1) a single, gradually propagating delamination (see Fig. 1c) and (2) fragmentation, which is defined here as multiple CFRPP fractures accompanied by delamination (see Fig. 1d). Fragmentation typically starts off as a single CFRPP failure and delamination, but as stress builds up again, new CFRPP failures appear instead of a growing delamination. In both cases, CFRPP failure may inflict damage to the SRPP layers.
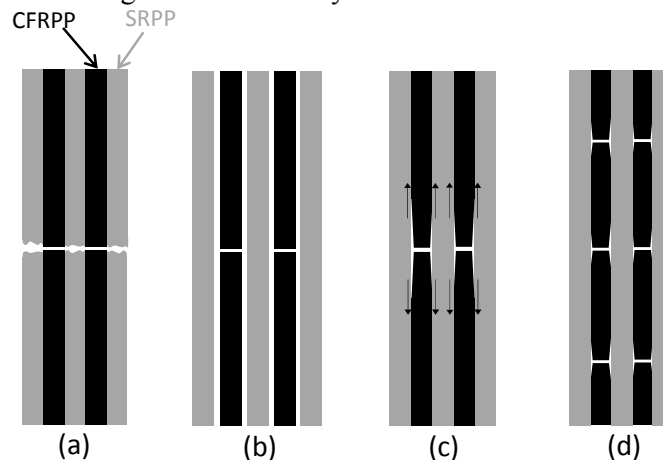

Figure 1: Schematic representation of the possible damage mechanisms in hybrid composites after failure of the two carbon fibre layers: (a) failure of the entire composite, (b) a delamination, which instantly develops to cover the entire specimen length, (c) a single, gradually propagating delamination, and (d) fragmentation or multiple CFRPP fractures accompanied by delaminations.

Four parameters will be varied to control the damage mechanisms: carbon fibre V_f, CFRPP and SRPP orientation and the relative thickness of the CFRPP layer. The interlaminar fracture toughness is missing from this list, but this value will be varied indirectly by changing the CFRPP and SRPP orientation.

5

3.2 Carbon fibre volume fraction

Fig. 2 presents the stress-strain diagrams of UD CFRPP - woven SRPP hybrids. The reference non-hybrid composites with 0%CF and 45%CF show drastically different behaviour. CFRPP is strong and stiff with a low failure strain, whereas SRPP is compliant, but has a high failure strain.

Both carbon fibre layers break simultaneously in the same location, as identified from post-mortem investigations. The tensile behaviour of the hybrids corresponds to the mechanism of a single, growing delamination around each broken carbon fibre layer (see Fig. 1c). This is also confirmed by the sample appearance of the 29%CF hybrid immediately before and after CFRPP failure (see Fig. 2b and c). The light grey regions correspond to the delaminations between the CFRPP and SRPP layers. Fig. 2d indicates that this delamination gradually grows upon further loading. At about 10% strain, the delamination covers the entire sample length. The sample then reverts to the situation of complete delamination (see Fig. 1b), where the SRPP layers are loaded independently from the fractured CFRPP layers. It should be noted that some damage is introduced into the SRPP, as the ultimate failure strain is slightly reduced compared to 0%CF. This reduction is smaller for lower carbon fibre V_f.
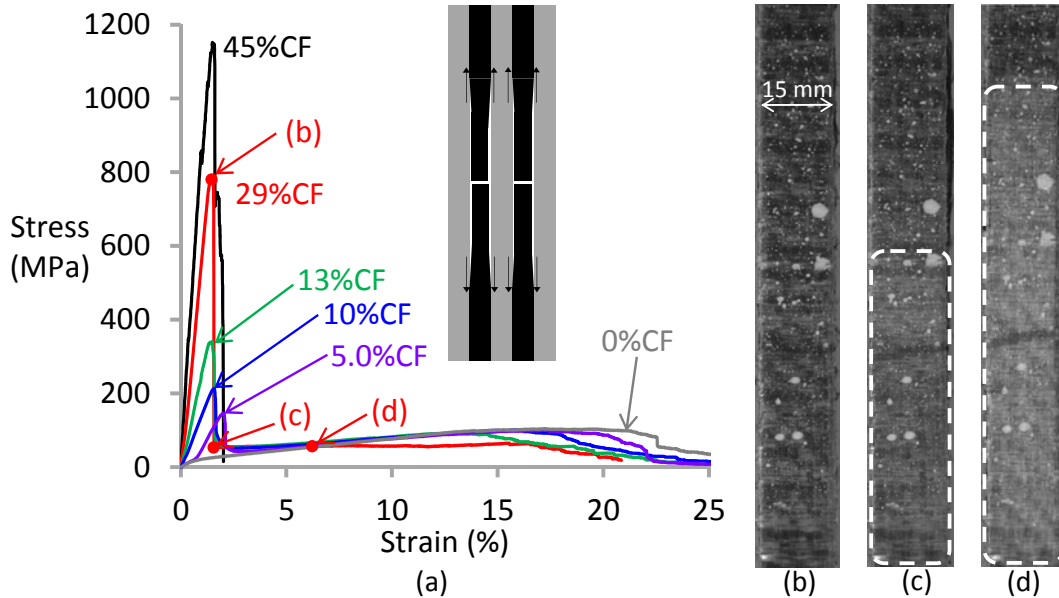

Figure 2: UD CFRPP – woven SRPP hybrid composites: (a) stress-strain diagrams along with those of the reference composites, (b) 29%CF sample right before CFRPP failure, (c) 29%CF sample immediately after CFRPP failure, and (d) 29%CF sample after 6% applied strain. The dashed rectangle indicates the delaminated region, whereas the white speckles are required for digital image correlation.

Immediately after CFRPP failure, the delamination length is 70 mm on average, corresponding to nearly half the gauge length. Such large delaminations should be avoided, as they lower the probability of complete stress build up in the CFRPP layers. This stress build up is vital for achieving multiple cracks or fragmentation. The large initial delaminations are facilitated by fibre debonding and splitting due to the low adhesion between carbon fibre and PP.

The available energy for creating delaminations is related to the energy that is stored in the CFRPP and released upon failure. This energy is the same for the 29%CF, 13%CF and 10%CF hybrids, as these layups all have the same number of carbon fibre plies (see Table 1). Their layups also ensure

6

that the number of surfaces that can delaminate is the same. Reducing V_f from 29% to 13% and 10% therefore did not change the general appearance of the stress-strain diagrams (see Fig. 2), nor did it change the initial delamination length. The only observed change is the fact that the SRPP ductility is maintained better for the 13%CF and the 10%CF hybrids. This is because these hybrids have more SRPP layers to absorb the released energy.

The 5.0%CF layup only has a single carbon fibre layer compared to 2 layers for the other layups (see Table 1). The lower elastic energy stored in this sample would hence be expected to have an effect on the delamination length. Unfortunately, visual detection of the delaminations was not possible due to the thick SRPP layers blocking the light too much. The damage to the SRPP was limited for all layups as the ultimate failure strain only increased slightly with decreasing carbon fibre V_f.

The 5.0%CF layup led to undulations in the carbon fibres, which cause nonlinearities in the range of 0-0.8% strain. The undulations occur due to entropic shrinkage of the PP tapes at high temperature, but also during cooling due to the large thermal expansion of SRPP [30, 31]. The carbon fibres are straightened before they fail, which is also indicated by the increased CFRPP failure strain (see Fig. 2). The undulations thus have only a minor influence on the damage mechanisms and are not studied here. Higher fractions of carbon fibre stabilise the CFRPP for these undulations and reduce the driving force for shrinkage by reducing the SRPP fraction.

The energy underneath the tensile diagrams was analysed, but did not show significant improvements compared to the linear rule-of-mixtures and was therefore not shown here.

3.3 Directionality of CFRPP

Reducing the carbon fibre V_f was insufficient to cause a change in the damage mechanism as the released energy and delamination length remained the same. Adding 90° carbon fibres is a well-known approach to hinder delamination, as it deflects and branches the delamination path, thereby increasing the interlaminar fracture toughness [32-34]. This section hence replaces the UD CFRPP layers with woven CFRPP to investigate its influence on the tensile behaviour. This also changes the stiffness and strength of the CFRPP layers.

Fig. 3 reveals that hybrids with woven CFRPP indeed behave differently. The initial delamination length is reduced to 30 mm (see Fig. 3c), compared to 70 mm for UD CFRPP (see Fig. 2c). This shows that 90° fibres are efficient in shortening the delamination. The delamination grows slightly, but then the SRPP layers start to fail. The SRPP always failed in the region where the CFRPP failed, indicating that CFRPP failure locally introduced damage into the SRPP layers.

Damage to the SRPP can be avoided by reducing the carbon fibre V_f (see Fig. 3). The energy that is released upon CFRPP failure remains the same for the 20%CF, 11%CF and 7.2%CF hybrids, as they have the same number of CFRPP layers. The lower V_f in the 7.2%CF layup however makes it more efficient in resisting damage to the SRPP.

Inspection of the initial delamination lengths revealed that they were consistently around 30 mm for the 20%CF, 11%CF and 7.2%CF hybrids. This is again related to the fact the number of CFRP layers and hence the released energy is the same. The delamination length seems to be even smaller for the 4.7%CF, but the contrast between delaminated and undelaminated regions was too low for accurate measurement.
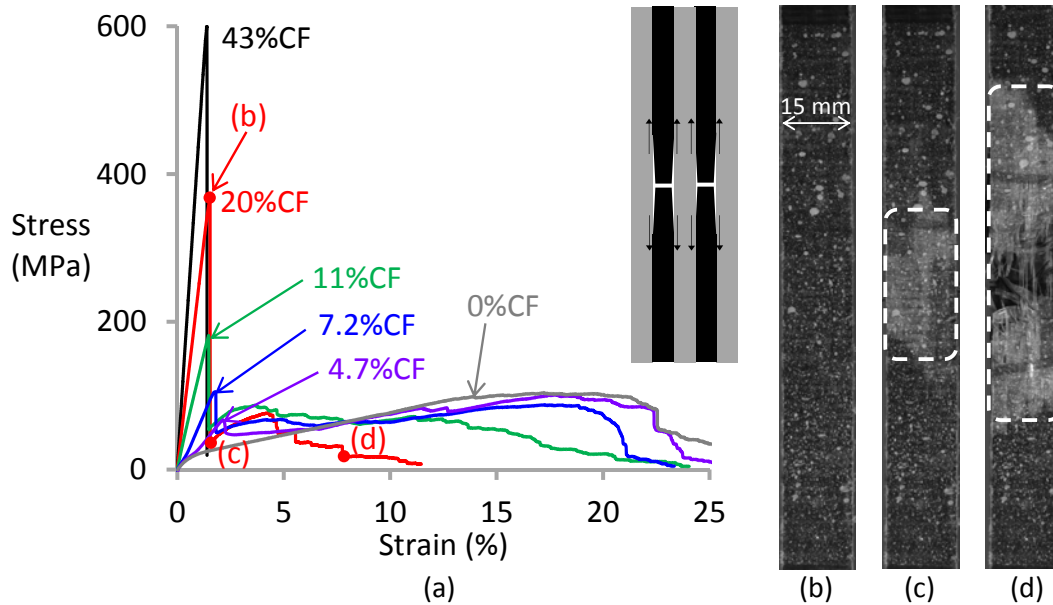
Figure 3: Woven CFRPP – woven SRPP hybrid composites: (a) stress-strain diagrams along with those of the reference composites, (b) 20%CF sample right before CFRPP failure, (c) 20%CF sample immediately after CFRPP failure, and (d) 20%CF sample at an applied strain of 8%. The dashed rectangle indicates the delaminated region.

3.4 Directionality of SRPP

The previous section highlighted the importance of carbon fibre orientation in hybrids with woven SRPP. The SRPP properties may also have an important effect on the performance and damage mechanisms of the investigated hybrids. This effect was investigated by using UD SRPP instead of woven SRPP, in combination with woven CFRPP. This increases both the stiffness and the strength of the SRPP, making it more appropriate to absorb the energy released by the CFRPP failure.

The 18%CF hybrids with UD SRPP (see Fig. 4) are able to maintain more of the SRPP ductility than the 20%CF hybrids with woven SRPP (see Fig. 3). Nevertheless, the mechanisms are similar in both hybrids: a single, gradually growing delamination around each CFRPP layer. Again, damage to the SRPP is reduced by lowering the carbon fibre V_f. The initial delamination length was 20-25 mm, irrespective of the carbon fibre V_f. This is shorter than the 30 mm in the woven CFRPP – woven SRPP hybrids. This is most likely related to the higher stiffness of the UD SRPP, but analysing the influence this has on the delamination is complex. Such analysis would require an energy-based approach, which will not be attempted here. This analysis should also be able to reveal why the delamination length was not lower for the 5.5%CF hybrid, even though this layup has fewer carbon fibre layers.
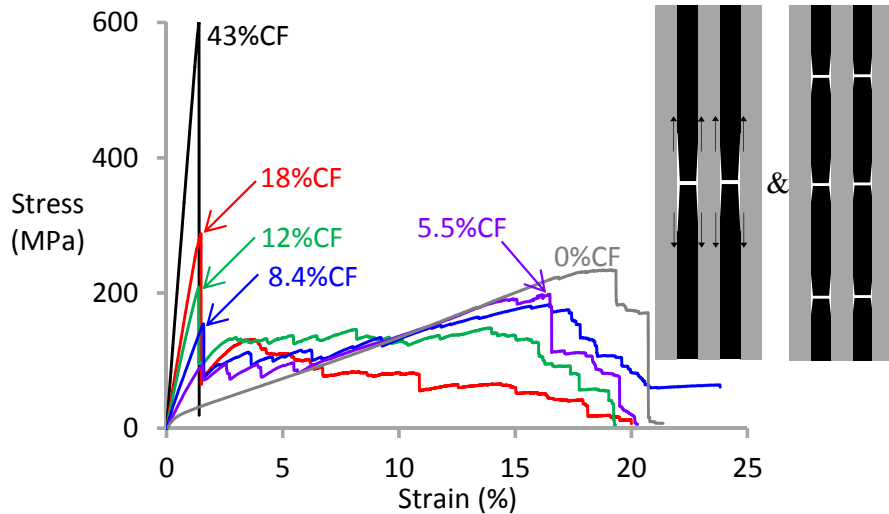
Figure 4: Stress-strain diagrams of woven CFRPP – UD SRPP hybrid composites with different carbon fibre volume fractions.

However, there is one vital difference: the 18%CF, 12%CF and 8.4%CF hybrids show a single growing delamination, whereas the 5.5%CF layups show fragmentation. Fig. 5 illustrates this behaviour in more detail. The tensile diagram in Fig. 5a displays four small peaks, followed by a larger one at about 15% strain. Fig. 5b shows the sample prior to the test. At this point, the material has a homogeneous colour. The white region in Fig. 5c develops after the first small load drop. This region indicates that the CFRPP has failed locally and is surrounded by a delamination. Further loading of the sample builds up stress, allowing the CFRPP layer to fracture again (see the second white region in Fig. 5d). This fragmentation occurred four times over the sample length, as illustrated in Fig. 5e. The delamination length was always 20-25 mm, irrespective of whether it was the first delamination.
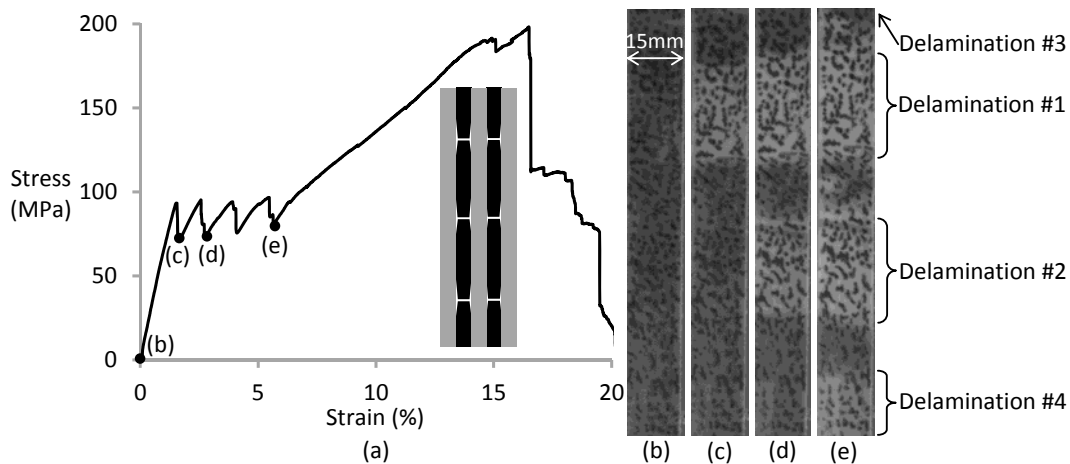

Figure 5: Illustration of the fragmentation behaviour in the 5.5%CF hybrids: (a) tensile diagram and sample (b) prior to failure, (c) after first fragmentation, (d) after second fragmentation, and (e) after the fourth and final fragmentation. The third fragmentation occurred outside of the imaged zone. The black speckles are used for digital image correlation.

The stress increase as a function of strain was synchronised with videos of the sample surface. The onset of the delaminations corresponds to the stress drops in the stress-strain curves. The multiple fractures of the CFRPP layers were confirmed by melting away the PP and observing the CFRPP layers. At about 6% strain, the CFRPP layers are completely delaminated, and SRPP becomes the only load carrying material.

3.5 Relative layer thickness

All 5.5%CF hybrids with woven CFRPP and UD SRPP fragmented, whereas none of the other described layups fragmented. Fragmentation prevents localisation of the strain and allows a higher stress level to be maintained. There is however a maximum relative layer thickness above which fragmentation does not occur anymore [14, 15]. To examine the upper limit, hybrid composites with a varying number of UD SRPP layers and a single woven CFRPP layer in the middle were produced. The carbon fibre V_f varied between 2.1% and 10% (see Table 2).

Table 2: The critical layer thickness and number of fragmented samples for the various layups. All these layups consist of woven CFRPP and UD SRPP.

Layup	Carbon fibre volume fraction		Total thickness (mm)	CFRPP thickness (mm)		Critical layer thickness (mm)	Number of fragmented samples
	Overall	in loading direction					
$S_{12}^U C^W S_{12}^U$	$2.1 \pm 0.1\%$	$1.0 \pm 0.1\%$	2.09 ± 0.03	0.104	$<$	0.147	5/5
$S_6^U C^W S_6^U$	$4.0 \pm 0.1\%$	$2.0 \pm 0.1\%$	1.11 ± 0.01	0.104	$<$	0.117	5/5
$S_5^U C^W S_5^U$	$4.6 \pm 0.6\%$	$2.3 \pm 0.3\%$	0.95 ± 0.01	0.104	$<$	0.111	5/5
$S_4^U C^W S_4^U$	$5.5 \pm 0.4\%$	$2.7 \pm 0.2\%$	0.79 ± 0.02	0.104	$\approx$	0.102	4/5
$S_3^U C^W S_3^U$	$7.0 \pm 1.6\%$	$3.5 \pm 0.8\%$	0.62 ± 0.01	0.104	$>$	0.093	1/5
$S_2^U C^W S_2^U$	$10.2 \pm 0.6\%$	$5.1 \pm 0.3\%$	0.43 ± 0.01	0.104	$>$	0.080	0/5

The stress-strain diagrams of these hybrid composites are shown in Fig. 6. All layups show peaks followed by vertical stress drops. These stress drops are either caused by sudden delamination growth or by fragmentation of the CFRPP layer. To determine whether fragmentation occurred (see Table 2), digital correlation images of the samples during the tensile tests were used to decide whether the samples fragmented.
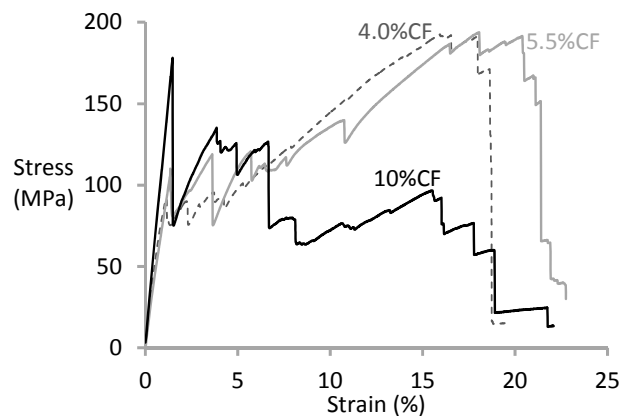

Figure 6: Representative stress-strain diagrams of woven CFRPP – UD SRPP hybrid composites with a single carbon fibre layer in the middle. Some layups were omitted to improve clarity.

Having a single instead of multiple CFRPP layers is required for the model in [14] to be applicable. The model therefore cannot applied to the layups used in the previous sections, as they contain multiple CFRPP layers. It should also be emphasised that the model does not predict anything related to the initial delamination length. This length is controlled by the energy released by the CFRPP failure and how this energy is distributed between SRPP damage and the creation of the initial delamination. Predicting this distribution is complex and will not be attempted here.

Czél and Wisnom's model [14] establishes an energy criterion for preventing the propagation of a delamination, which is necessary to achieve fragmentation. This criterion is based on changes in the elastic strain energy before and after the CFRPP layer fails. The critical layer thickness t_{CFRPP}^c is found when this energy change is equal to the energy required to cause delamination of the central CFRPP layer. This assumes that delamination is the only energy absorbing mechanism and leads to the equation:

$$G_{II,C} = \frac{\sigma_{CFRPP}^2 \cdot t_{CFRPP}^c \cdot \left(E_{SRPP} \cdot \left(t - t_{CFRPP}^c \right) + E_{CFRPP} \cdot t_{CFRPP}^c \right)}{4 \cdot E_{SRPP} \cdot E_{CFRPP} \cdot \left(t - t_{CFRPP}^c \right)}, \qquad (1)$$

where $G_{II,C}$ is the mode II interlaminar fracture toughness for propagation, σ_{CFRPP} is the strength of the central CFRPP layer, E_{SRPP} and E_{CFRPP} are the tensile moduli of the SRPP and CFRPP layers respectively, and t is the total sample thickness.

All required input parameters are available from the tensile tests, apart from $G_{II,C}$. This value is challenging to measure due to the low CF/PP adhesion and the low stiffness of hybrid composites. Since CFRPP is not a common prepreg, the amount of literature on its $G_{II,C}$ is limited. Taketa [35] quoted values of 0.497 ± 0.026, 0.674 ± 0.017 and 0.384 ± 0.010 kJ/m² for fast, medium and slowly cooled UD CFRPP. Since no consistent trend can be observed, the average value of 0.518 kJ/m² was used. This is very close to 0.514 kJ/m² reported by Hu [36]. These values have two important caveats. Firstly, the CFRPP prepregs used by Taketa and Hu may have a different PP matrix. Secondly, they reported $G_{II,C}$ values for UD CFRPP, while the equation will be applied to woven CFRPP hybrids. The $G_{II,C}$ is typically higher for woven than for UD composites [37].

The number of fragmented samples for each layup was counted from the photographs. All these results are summarised in Table 2. The number of fragments in the fragmented samples varied between 2 and 4, but did not seem to depend on the layup. While 4/5 samples of the 5.5%CF hybrid still fragment, only 1 out 5 samples of 7.0%CF hybrid did. The critical carbon fibre V_f is hence around 6%CF in the experiments, and samples do not fragment anymore at higher V_f. This corresponds to a relative woven layer thickness of 13% or 3%CF in the loading direction.

Eq. 1 was solved using the appropriate values for CFRPP and SRPP. The predicted critical layer thickness t_{CFRPP}^c depends on the layup, as the sample thickness t was each time adapted to the thickness of the specific layup. The actual CFRPP thickness should be smaller than the critical layer thickness to prevent delamination propagation. This is required to achieve fragmentation (see Fig. 1d) instead of a growing delamination (see Fig. 1c). Table 2 proves that the predictions correspond well with the experimental data.

As the $G_{II,C}$ value was taken from literature, analysing its significance for the critical layer thickness is a useful exercise. The critical layer thickness indeed seems to be sensitive to the fracture toughness (see Fig. 7). Using either 0.4 or 0.6 kJ/m² for $G_{II,C}$ would change the critical layer

thickness by about 15%. These small variations would change the comparison with the presented experimental data (see Table 2).
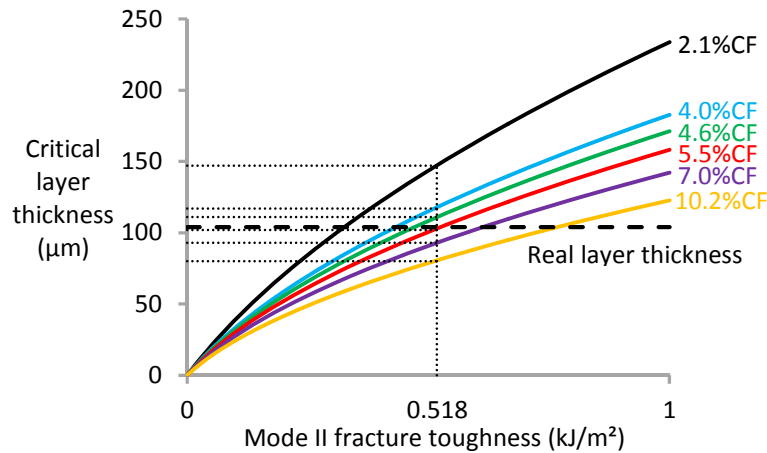

Figure 7: Prediction of the critical layer thickness from the model of Czél and Wisnom [14].

4 Conclusion

CFRPP/SRPP hybrid composites combine a tensile modulus of 10-20 GPa with an ultimate failure strain of 20%. The damage mechanisms in these hybrids were analysed and the influence of various parameters was demonstrated:

- The amount of carbon fibre and its V_f determine the amount of the damage to the SRPP, but does not necessarily affect the delamination length.
- Woven CFRPP leads to a shorter delamination length than UD CFRPP.
- UD SRPP leads to less damage in the SRPP than in woven SRPP and also facilitates fragmentation.
- Fragmentation was achieved for relative woven CFRPP layer thicknesses below 14% in UD SRPP hybrids. The highest carbon fibre V_f that still achieves fragmentation is about 6%, of which half is in the loading direction.

The mechanical performance of CFRPP/SRPP hybrids can be optimised by an intelligent combination of these parameters. These conclusions can also be used to control the damage mechanisms and achieve ductility in other hybrid composites.

5 Acknowledgements

6 References

[1] Swolfs Y, Crauwels L, Gorbatikh L, Verpoest I. The influence of weave architecture on the mechanical properties of self-reinforced polypropylene. Composites Part A: Applied Science and Manufacturing. 2013;53:129-36.

[2] Swolfs Y, Zhang Q, Baets J, Verpoest I. The influence of process parameters on the properties of hot compacted self-reinforced polypropylene composites. Composites Part A: Applied Science and Manufacturing. 2014;65:38-46.

[3] Swolfs Y, Van den fonteyne W, Baets J, Verpoest I. Failure behaviour of self-reinforced polypropylene at and below room temperature. Composites Part A: Applied Science and Manufacturing. 2014;65:100-7.

[4] Callens MG, Gorbatikh L, Verpoest I. Ductile steel fibre composites with brittle and ductile matrices. Composites Part A: Applied Science and Manufacturing. 2014;61:235-44.

[5] Callens MG, Gorbatikh L, Bertels E, Goderis B, Smet M, Verpoest I. Tensile behaviour of steel fibre/epoxy composites with modified adhesion. Composites Part A: Applied Science and Manufacturing. 2015;69:208-18.

[6] Espinosa HD, Rim JE, Barthelat F, Buehler MJ. Merger of structure and material in nacre and bone - Perspectives on de novo biomimetic materials. Progress in Materials Science. 2009;54:1059-100.

[7] Peterlik H, Roschger P, Klaushofer K, Fratzl P. From brittle to ductile fracture of bone. Nature Materials. 2006;5:52-5.

[8] Gorbatikh L, Lomov SV, Verpoest I. Original mechanism of failure initiation revealed through modelling of naturally occurring microstructures. Journal of the Mechanics and Physics of Solids. 2010;58:735-50.

[9] Ebacher V, Wang R. A Unique Microcracking Process Associated with the Inelastic Deformation of Haversian Bone. Advanced Functional Materials. 2009;19:57-66.

[10] Barthelat F, Espinosa HD. An experimental investigation of deformation and fracture of nacre-mother of pearl. Experimental Mechanics. 2007;47:311-24.

[11] Rim JE, Zavattieri P, Juster A, Espinosa HD. Dimensional analysis and parametric studies for designing artificial nacre. Journal of the Mechanical Behavior of Biomedical Materials. 2011;4:190-211.

[12] Li VC. Can Concrete Be Bendable? The notoriously brittle building material may yet stretch instead of breaking. American Scientist. 2012;100:484-93.

[13] Bunsell AR, Harris B. Hybrid carbon and glass fibre composites. Composites. 1974;5:157-64.

[14] Czél G, Wisnom MR. Demonstration of pseudo-ductility in high performance glass/epoxy composites by hybridisation with thin-ply carbon prepreg. Composites Part A: Applied Science and Manufacturing. 2013;52:23-30.

[15] Jalalvand M, Czél G, Wisnom MR. Numerical modelling of the damage modes in UD thin carbon/glass hybrid laminates. Composites Science and Technology. 2014;94:39-47.

[16] Dai G, Mishnaevsky Jr L. Fatigue of hybrid glass/carbon composites: 3D computational studies. Composites Science and Technology. 2014;94:71-9.

[17] Enfedaque A, Molina-Aldareguia JM, Galvez F, Gonzalez C, Llorca J. Effect of Glass Fiber Hybridization on the Behavior Under Impact of Woven Carbon Fiber/Epoxy Laminates. Journal of Composite Materials. 2010;44:3051-68.

[18] Swolfs Y, Gorbatikh L, Verpoest I. Stress concentrations in hybrid unidirectional fibre-reinforced composites with random fibre packings. Composites Science and Technology. 2013;85:10-6.

[19] Swolfs Y, Gorbatikh L, Verpoest I. Fibre hybridisation in polymer composites: a review. Composites Part A: Applied Science and Manufacturing. 2014;67:181-200.

[20] Yeter E, Erklig A, Bulut M. Hybridization effects on the buckling behavior of laminated composite plates. Composite Structures. 2014;118:19-27.

[21] González EV, Maimí P, Sainz de Aja JR, Cruz P, Camanho PP. Effects of interply hybridization on the damage resistance and tolerance of composite laminates. Composite Structures. 2014;108:319-31.

[22] Ilbeom C, Dongyoung L, Dai Gil L. Hybrid composite low-observable radome composed of E-glass/aramid/epoxy composite sandwich construction and frequency selective surface. Composite Structures. 2014;117:98-104.

[23] Swolfs Y, McMeeking RM, Gorbatikh L, Verpoest I. The effect of fibre dispersion on initial failure strain and cluster development in unidirectional carbon/glass hybrid composites. Composites Part A: Applied Science and Manufacturing. 2015;69:279-87.

[24] Swolfs Y, Crauwels L, Van Breda E, Gorbatikh L, Hine P, Ward I, et al. Tensile behaviour of intralayer hybrid composites of carbon fibre and self-reinforced polypropylene. Composites Part A: Applied Science and Manufacturing. 2014;59:78-84.

[25] Hine P, Bonner M, Ward I, Swolfs Y, Verpoest I, Mierzwa A. Hybrid carbon fibre/nylon 12 single polymer composites. Composites Part A: Applied Science and Manufacturing. 2014;65:19-26.

[26] Verpoest I, Lomov S, Swolfs Y, Jacquet P, Michaud V, Manson J-A, et al. Advanced materials enabling high-volume road transport applications of lightweight structural composite parts. Sampe Journal. 2014;50:30-7.

[27] Ward IM, Hine PJ. The science and technology of hot compaction. Polymer. 2004;45:1413-27.

[28] Múgica JI, Aretxabaleta L, Ulacia I, Aurrekoetxea J. Impact characterization of thermoformable fibre metal laminates of 2024-T3 aluminium and AZ31B-H24 magnesium based on self-reinforced polypropylene. Composites Part A: Applied Science and Manufacturing. 2014;61:67-75.

[29] Carrillo JG, Cantwell WJ. Mechanical properties of a novel fiber-metal laminate based on a polypropylene composite. Mechanics of Materials. 2009;41:828-38.

[30] Le Bozec Y, Kaang S, Hine PJ, Ward IM. The thermal-expansion behaviour of hot-compacted polypropylene and polyethylene composites. Composites Science and Technology. 2000;60:333-44.

[31] Taketa I, Ustarroz J, Gorbatikh L, Lomov SV, Verpoest I. Interply hybrid composites with carbon fiber reinforced polypropylene and self-reinforced polypropylene. Composites Part A: Applied Science and Manufacturing. 2010;41:927-32.

[32] Ogasawara T, Yoshimura A, Ishikawa T, Takahashi R, Sasaki N, Ogawa T. Interlaminar Fracture Toughness of 5 Harness Satin Woven Fabric Carbon Fiber/Epoxy Composites. Advanced Composite Materials. 2012;21:45-56.

[33] Alif N, Carlsson LA, Boogh L. The effect of weave pattern and crack propagation direction on mode I delamination resistance of woven glass and carbon composites. Composites Part B-Engineering. 1998;29:603-11.

[34] Kotaki M, Hamada H. Effect of interfacial properties and weave structure on mode I interlaminar fracture behaviour of glass satin woven fabric composites. Composites Part A: Applied Science and Manufacturing. 1997;28:257-66.

[35] Taketa I. Analysis of failure mechanisms and hybrid effects in carbon fibre reinforced thermoplastic composites [PhD. thesis]. Leuven: KU Leuven, 2011.

[36] Hu Y. Micromechanics of chopped fiber composites using carbon fiber and thermoplastic matrix [Master thesis]. Leuven: KU Leuven, 2010.

[37] Compston P, Jar PYB. Comparison of Interlaminar Fracture Toughness in Unidirectional and Woven Roving Marine Composites. Applied Composite Materials. 1998;5:189-206.